Journal of Physics: Conference Series **528** (2014) 012009 doi:10.1088/1742-6596/528/1/012009

Using Parabolic Supermirror Lenses to Focus and De-focus a Neutron Beam

Emmanouela Rantsiou[1], Tobias Panzner[1], Patrick Hautle[1], Uwe Filges[1]

[1]Paul Scherrer Institute, Laboratory for Developments and Methods, 5232 Villigen PSI, Switzerland

E-mail: emmanouela.rantsiou@psi.ch

Abstract. We designed a focus/defocus neutron optics system, in order to investigate the performance, precision, efficiency, and operational and designing challenges of such coupled 2-lens systems, which could potentially find applications where small beam cross sections are beneficial, e.g., virtual neutron source concepts and high efficiency chopper systems. Our particular prototype (as described and discussed in this paper) has already been used in an on-going experiment, involving neutron spin filtering with dynamically polarized protons.

After the designing and construction phases, we continued by performing a long series of simulations and measurements, in order to facilitate the alignment of the lenses, and investigate and understand the behaviour and output of the system. All measurements were performed at the BOA beamline at PSI. The simulations were particularly useful in aligning the lenses: tilts as small as 0.04° could easily be accounted for in our simulations and guide successfully the experimental aligning procedure of the first lens. Although harder to do in the case of two lenses, we were still able to reproduce fairly successfully with our simulations, tilts from both lenses. We have noticed (both in our experiments and simulations) that the sensitivity of such a set-up is $\sim 0.01^\circ$.

1. Introduction

Ever since supermirrors were proposed and built [1, 2, 3], they have found numerous applications in transporting, bending, focusing and polarizing neutron beams. Supermirror technology makes use of multilayer depth-graded coatings (most commonly of Ni and Ti) in order to increase the critical angle of reflection of the mirror by a factor m compared to that of natural ^{58}Ni. Looking at the definition of that factor $m = \theta_c/\theta_c^{Ni}$, with $\theta_c^{Ni} = 0.1^\circ/\mathring{A}$, it becomes apparent that the longer the wavelength of the incident neutron, the higher the reflectivity (i.e., the probability of it being reflected), as the divergence tolerance increases with wavelength. Nowadays, supermirrors exhibit reflectivity above 80% for $m \leq 4$, but that value drops to 50% as their coating reaches $m = 7$. A thorough discussion on technicalities of supermirror development can be found in [4].

With technological advances allowing for construction of supermirrors with higher m values, improved reflectivity, and new shapes (elliptical and parabolic), and also ongoing theoretical work on supermirrors, which has been greatly facilitated by simulations, more uses of supermirrors are becoming apparent. The idea of using supermirror lenses to focus and defocus a neutron beam has begun being investigated and tested over the last few years [5, 6]. In this paper we present a proof-of-principle project, carried out at PSI, on the performance and overall

behaviour of a 2-lens focus/defocus system.

2. Conceptual Phase and Simulations

The purpose of this project has been to investigate the use of parabolic supermirror neutron lenses in a focus-defocus system, starting from the initial design phase, and following through with the experimental set up and measurements. Besides our interest in the behaviour, sensitivity, efficiency and experimental outcome of such a coupled lens system, we were particularly focused on determining whether simulations can function not only as designing tools, but also reliably guide and correct the alignment of the two lenses during the experiment.

We began by designing the two lenses and determining their characteristics using the Monte Carlo Ray-tracing software McStas [7, 8]. Here we had to take into account that the behaviour and performance of these prototypes should be explored in conjunction with a potential application: a novel neutron spin filter using DNP (Dynamic Nuclear Polarization) [9]. The specifics of that experiment dictated to a certain extent the characteristics and dimensions that the two lenses should have. For example, the defined sample size for use in the DNP experiment was only $\sim 5 \times 5\,\mathrm{mm}^2$, it should be placed as close to the exit of the focusing lens as possible (to maximize intensity), but not closer than $\sim 200 - 250\,\mathrm{mm}$ due to restrictions from equipment placed around the sample. Furthermore, at the sample position the focusing lens (hereafter L1) should provide spatially homogeneous intensity, while the defocusing lens (hereafter L2), placed after the sample, should be able to accept as much as possible of the neutrons coming through the sample and restore the original beam properties. All the above, combined with considerations on costs for the prototype, resulted after several rounds of simulations and optimizations in two lenses whose characteristics are presented on Table 1. L2 is ideally identical to L1 (turned 180° to serve as a defocusing lens), but we ended up constructing only half of it (thus its 0.5 m length), as a full defocusing lens was not really necessary for these preliminary, proof of principle experiments. In our simulations however, we integrated both the half-meter and the one-meter L2 lens, as it is obvious from the results presented on Table 2.

Table 2 shows simulated intensity and divergence values at various crucial positions along the 2-lens set up, for 3 different configurations for L2: i) full one-meter length, placed 0.8 m after L1, ii) full one-meter length, placed 0.5 m after L1, iii) half-meter length, placed 0.5 m after L1. At the first configuration, the focal points of L2 and L1 are at the same position, midway between the two lenses (both lenses have a focal point of 0.4 m). At the second and third configuration (denoted as 'defoc'), L2 is positioned closer to L1, 'looking' 0.3 m before the focal point of L1. Also, in all cases we have used slits before L1 (but also before L2), in order to make sure that a) the full entrance of L1 is illuminated and b) no neutrons pass around L1, contaminating either L2 or making their way onto our final CCD images.

As indicated by the results summarized on Table 2, L1 exhibits a neutron transport of 87% for a white beam ($1 - 10\mathring{A}$) of $\sim 0.5°$ divergence. 22% of those transported neutrons are focused on a $5 \times 5\,\mathrm{mm}^2$ area at the focal point of the focusing lens, with the divergence increased to $\sim 1.3°$. About 37% to 76% of the neutrons transported by L1 are passed through to L2, depending on the position of L2, as it is seen by the two intensity values listed for the entrance of L2. This seemingly low value of intensity transfer between the two lenses can be attributed to the divergence of the direct beam, connected to the relatively large distances, and aberration effects. Aberration alone accounts for up to 30% of intensity loss. As mentioned earlier, our lenses were optimized for providing homogeneous intensity distribution on a $5 \times 5\,\mathrm{mm}^2$ target at 200 mm after L1, and not as a stand alone focus-defocus lens, in which case, the losses in neutrons transferred among the two lenses could be lowered to $10 - 15\%$.

Finally, the length and position of L2 change significantly (as expected) its intensity output and the outcoming neutrons' divergence. For example, increasing the length of L2 restores the initial divergence of the beam, on the expense of intensity. On the other hand, moving L2

closer to L1 (configurations ii and iii) boosts up intensity, but doesn't quite manage to lower the divergence as efficiently as the third configuration.

We mention here that the option to 'defocus' L2 came out of the optimization of the system for the needs of the DNP experiment: we opted for higher intensity input for L2, at the expense of the restored divergence of the beam.

Table 1. Characteristics of the two prototype lenses.

	Focusing Lens (L1)	Defocusing Lens (L2)
Shape	(trully-shaped) parabolic	(trully-shaped) parabolic
Length $[mm]$	1000	500
Entrance size $[mm^2]$	25×25	13.363×13.363
Exit size $[mm^2]$	13.363×13.363	20.04×20.04
m	3.6	3.6
focal point $[mm]$	400 (after L1 exit)	400 (before L2 entrance)
gain factor[1]	$7.5 - 11$	–

Table 2. Characteristic intensity and divergence values from simulations

	Intensity $[n/s/mA]$	Divergence [°] (horizontal/vertical)
L1 entrance	2.34×10^8	0.5/0.4
L1 exit	2.04×10^8	1.3/1.2
200mm after L1 [2]	5.4×10^7	1.3/1.2
Focal point[2]	4.55×10^7	1.3/1.2
L2 entrance	7.08×10^7	1.3/1.2
L2 entrance (defoc)	1.55×10^8	1.3/1.2
(full) L2 exit	5.17×10^7	0.55/0.45
(full) L2 exit (defoc)	8.68×10^7	0.7/0.7
(half) L2 exit (defoc)	1.11×10^8	0.9/0.9

3. Experimental Phase: Measurements and Simulations

After the construction of the lenses was complete, we proceeded to perform experiments at the BOA beamline at PSI. Our experimental procedure was divided in two steps: i) the placement and alignment of the lenses in the beamline one after the other, and ii) testing and investigating the performance and outcome of the complete 2-lens system for various configurations, i.e. varying the relative lens distances and orientations, usage of slits, etc. The lenses were placed on separate motorized stages that could move along the direction of the beam path, and also rotate horizontally and vertically with respect to the axis of the lens. Furthermore, both lenses were equipped with microscrews mounted on their holders, enabling for very small inclination

[1] Wavelength dependent
[2] On an area of $5 \times 5mm^2$

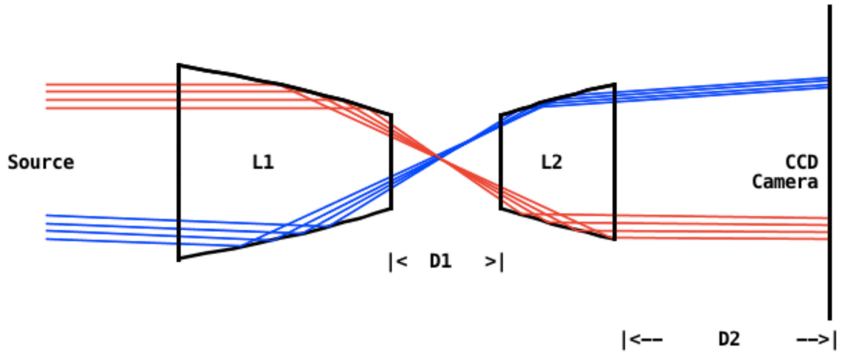

Figure 1. A schematic representation of our experimental setup. The focusing (L1) and defocusing (L2) lenses are shown, along with two groups of rays: parallel rays (upper group), and divergent rays (lower group). The distance D1 between the two lenses as well as the distance D2 between the defocusing lens and the CCD camera, were varying in our simulations and experiments. Relevant scales, ratios and sizes have been exaggerated for illustration purposes.

adjustments. A CCD camera was mounted on a third motorized stage, with the ability to move along the beamline, positioning the camera at various distances from the lenses. All results (experimental and simulated) presented here are for a white neutron beam. During all steps of the experimental procedure, extended simulation runs were performed in order to verify and guide our experiments.

3.1. Measurements and Simulations for the Focusing Lens

We began the experiments by placing and aligning the focusing lens L1 into the beamline. After an initial 'approximate' alignment with the use of a laser beam and a common light bulb, we finalised the alignment of L1 using the full neutron beam, performing scan measurements along the flightpath of the neutrons and correcting the position of L1 accordingly. McStas simulations were particularly helpful in the alignment procedure as the following representative example demonstrates.

At some point during the alignment of L1, the 1D intensity profile of the neutron beam in the Y-direction (up-down direction with respect to the path of the neutrons) as captured by the CCD camera, featured an asymmetry (Fig. 2(a)). Using McStas, we were able to reproduce that feature in our simulations, by introducing an upward tilt of the lens of 0.06°. Fig. 2(b) shows the simulated profiles (X- and Y-direction) for a perfectly aligned lens, and Fig. 2(c) shows the simulated profiles for the tilted lens. We were then able to correct our experimental set-up by tilting L1 0.06° downwards, and finalise its alignment.

Fig. 3 shows the 2-dimensional neutron intensity distributions after the alignment of L1 was completed, at two positions after L1: 200mm (panels (a) and (c)) and at the focal point (400mm) (panels (b) and (d)). Plots (a) and (b) correspond to the experimental images and plots (c) and (d) are result of simulations. We notice an excellent agreement between the experimental and simulated images, also highlighted on the results presented in Fig. 4: after we were convinced that L1 was aligned to a satisfactory level (through extensive measurements and comparison to simulations), we performed some measurements where we introduced a tilt of the lens (either in the horizontal of vertical direction), in order to quantify the sensitivity of our first lens to such misalignments. The upper row of Fig. 4 shows the 2D neutron intensity (experimental (a) and simulated (b)) distribution, 200mm after L1 and with L1 tilted by 0.2° to the right, relative the the neutrons' path. We notice a dramatic change of the intensity distribution profiles, due to a relatively small misalignment when we compare Figs. 4(a) and 4(b) to Figs. 3(a)

and 3(c) respectively. Plot (c) of Fig. 4 shows the one-dimensional horizontal profiles of the 2D distributions. The agreement between simulation and experiment is excellent: besides the match in the shape of the two curves, we notice that the length-scales of the two lines agree very well, and so do their relative intensity changes.

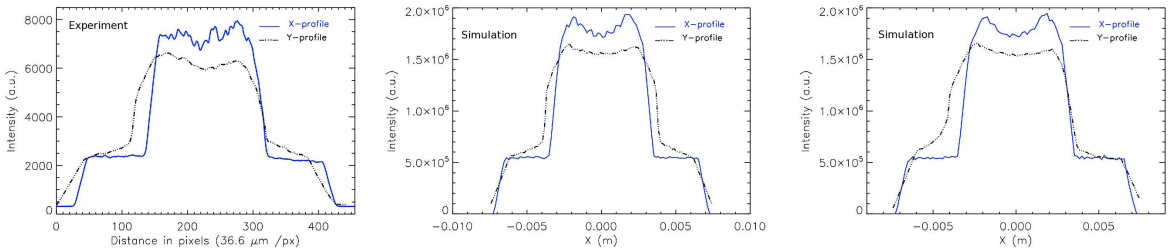

(a) (b) (c)

Figure 2. (a) Experimental 1D intensity profiles of L1 in X- and Y-directions. The Y-profile features an asymmetry: a bulging and a shift to the left, due to an accidental tilt of L1. (b) Simulated 1D intensity profiles of L1 in X- and Y-directions, for a perfectly aligned lens. (c) Simulated 1D intensity profiles of L1 in X- and Y-directions after introducing a 0.06° upward tilt of L1. Measurement and simulations correspond to a distance of 200mm after L1.

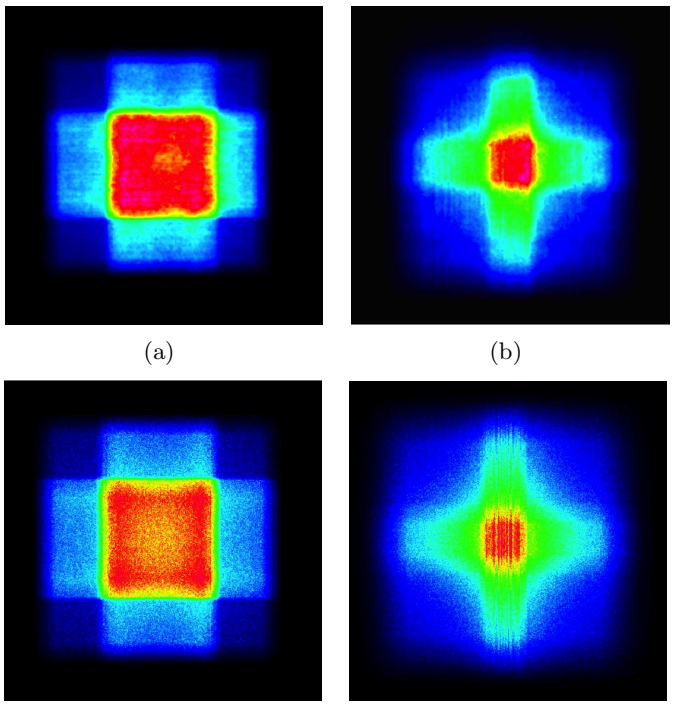

(a) (b) (c) (d)

Figure 3. Experimental (panels (a) and (b)) and simulated (panels (c) and (d)) 2D Neutron intensity distributions at 200mm ((a) and (c)) and 400mm - focal point ((b) and (d)) after L1.

3.2. Focusing and De-focusing Lenses Setup

With L1 nicely aligned, we introduced the defocusing lens L2 into the beamline and began its alignment. Simulations were again successfully used to correct and guide the procedure. With

both lenses aligned we performed scan measurements along the beam path with the CCD camera covering a range of distances between 300mm-2000mm from the exit of L2. We also performed inclination scans, were L2 was rotated vertically (up-down) and horizontally (left-right) from its aligned position, in order to quantify the effect of tilts of L2 on our set up.

Fig. 5 shows experimental (rows 1 and 3) and simulated (rows 2 and 4) 2D intensity distributions for three different positions after L2 (400mm, 1100mm, and 2000mm). The two lenses are 500 mm apart on the plots of the two upper rows and 800 mm apart on the plots of the two lower rows.

In Fig. 6 we show an example of the defocusing lens: as part of our experiments, L2 was rotated vertically (up-down direction) within a range of angles. Panel (a) of Fig. 6 shows the 1D intensity profile 300 mm after the exit of L2, for a 'downwards tilt' of 0.04°. Panel (b) of the same figure, was out attempt to simulate the effect of such a tilt. The match between experiment and simulation, even for such a small angle, is remarkable.

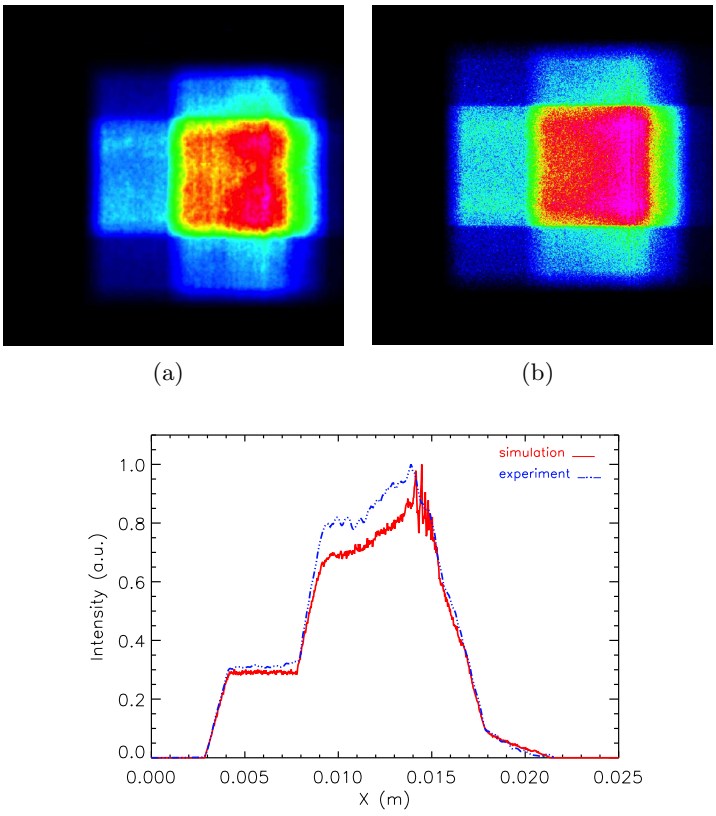

(a) (b)

(c)

Figure 4. *Up:* 2D neutron intensity distributions, 200mm after L1. The lens was tilted towards the right (relatively to the neutrons' direction) by 0.2°. Panel (a) shows the experimental result and panel (b) the simulated one. *Down:* 1D horizontal profiles of the plots in the upper row. Notice how precisely the simulation matches the experimental result, not only in the overall shape of the 1D profiles, but also the sizes of their features, and the relative increase of the central peak within each plot.

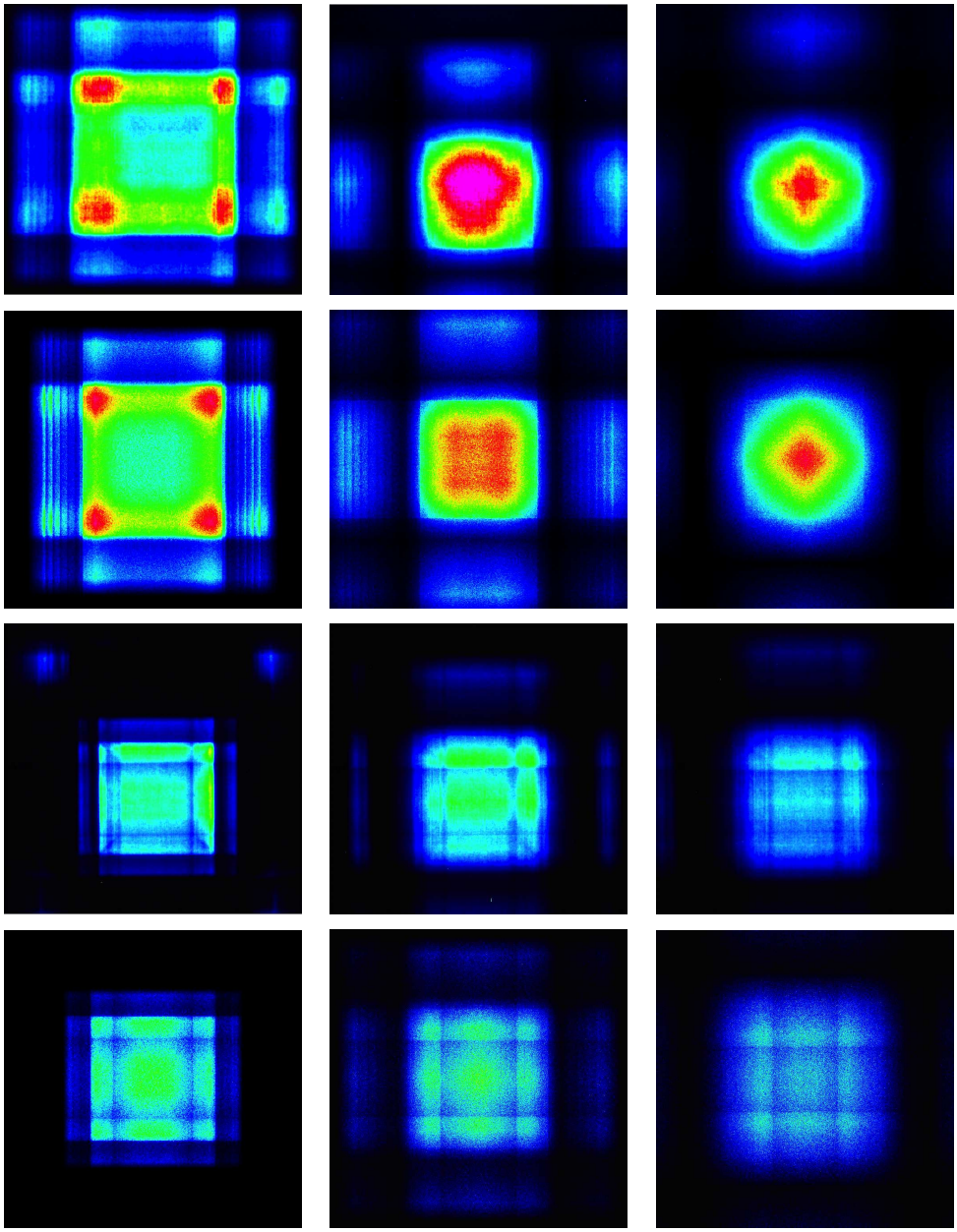

Figure 5. Experimental (rows 1 and 3) and simulated (rows 2 and 4) 2D intensity distributions in various distances from L2: 400mm (left), 1100mm (centre) and 2000mm (right) after L2. L2 was placed 500 mm after L1 for the plots on rows 1 and 2, and the distance was increased to 800 mm for the plots of rows 3 and 4

4. Summary

We have designed, built and tested a focus-defocus, 2-lens system, using parabolic supermirrors. We used McStas not only to simulate the two lenses during the designing phase, but also as a tool to guide us through the experimental alignment and testing. The simulations have proven to be a valuable tool for the alignment procedure, being able to successfully and reliably reproduce effects of misalignments as small as 0.04°. Generally speaking, we noticed that the system of the 2 lenses was sensitive to tilts of the order of 0.01°, making its alignment a tedious, non-trivial

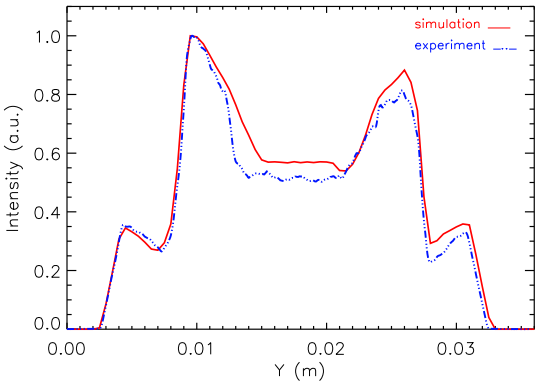

Figure 6. Simulated and experimental 1D intensity profiles in Y-direction, at 300 mm after L2. The two lenses were placed 500 mm apart. In our experimental set up, L2 was tilted downwards by 0.04°. Our simulations were able to reproduce the effect of the tilt very successfully.

task, which however is possible and can greatly benefit from simulations. On this note, as a follow-up to this project, we are currently planning the design of an 'automatic alignment tool', where camera images and simulations are used simultaneously, to provide real-time feedback to the lenses' motors, and thus spead-up and automatize the alignment procedure for coupled lens systems.

Acknowledgments

This project was funded by the European Spallation Source

References

[1] Turchin V F 1967 *At. Energy* 22
[2] Mezei F 1976 *Comm. Phys.* **1** 81
[3] Mezei F and Dagleish P A 1977 *Comm. Phys.* **2** 41
[4] Erko A, Idir M, Krist T and Michette A G (eds) 2008 *Neutron Supermirror Development* (Berlin-Heidelberg: Springer)
[5] Böni P 2007 *NIMPA* **586** 1
[6] Desert S, Panzner T and Permingeat P 2013 *J. Appl. Cryst.* **46** 35
[7] Lefmann K and Nielsen K 1999 *Neutron News* **10** 20
[8] Willendrup P, Farhi E and Lefmann K 2004 *Physica B* **350** 735
[9] Eichhorn T, Niketic N, van den Brandt B, Hautle P and Wenckebach W T *Proc., International Workshop on Neutron Optics and Detectors (NOP&D) 2013 Munich(Ismaning)*